Parametric Approach for Wide Field of View Multi-Projector Displays

Masato Ogata,† Hiroyuki Wada,† Kagenori Kajihara,†
Jeroen van Baar †† and Ramesh Raskar ††,†††

In this paper, we describe techniques for supporting wide field of view multi-projector curved screen display system. Our main contribution is in achieving automatic geometrical calibration and efficient rendering for seamless displays in presence of panoramic surround screens. We show several prototype systems which use a stereo camera for capturing and rendering on quadric curved screens. Due to a parameterized representation, the unified calibration method is independent of pose and field of view of the calibration camera. The method can simplify tedious and complicated installation and maintenance of large multi-projector displays in planetariums, virtual reality and visualization venues.

1. Introduction

The image distortion correction methods using computer vision can be divided into non-parametric and parametric approaches. For the non-parametric approach, the screen may be of arbitrary shape, while for the parametric approach the screen is restricted to the class of surfaces that can be expressed by mathematical functions. In [BAAR03][2),[RASK04][6) the authors explain the benefits of the parametric approach, specifically the accuracy of the alignment using low-cost cameras, and the possibility of head tracking. Although the methods are restricted to the group of quadratic surfaces, the most common display surfaces, e.g., planar, spherical and cylindrical surfaces, belong to that group.

In non-parametric approaches [YAMA02][4), [HASH04][5) , a camera is typically located in the eye position during calibration. In some cases, for example in flight simulators, mock-up hardware limits the available camera locations and makes accurate calibration in the non-parametric approach more difficult. In [RASK03][1) , the authors explain that for the parametric case the camera can be located in a different location, and moved virtually to the desired location. In [OGAT06][3) that desired location is computed from the parametric description of the underlying surface. This calibration is called *virtual camera method*, because there is no need to mount the camera exactly at the eye point, rather the camera can be mounted at an appropriate location in calibration.

In both [RASK03][1) and [OGAT06][3) , displays that fit within the cameras' field of view can be calibrated. This severely limits the displays' field of view.

2. *Virtual camera method*

We briefly describe the *virtual camera method* to introduce into a main theme of the paper. A principal idea of correcting image distortion in the method is to apply an inverse of the distortion caused by projection on the screen.

Calculation of inverse distortion is equivalent to find a mapping function $\boldsymbol{\Psi}_{p_i c}$ from a pixel position $\boldsymbol{x}_c$ in the camera to a corresponding pixel position $\boldsymbol{x}_{p_i}$ in the projector i,where suffix p_i indicates projector i, and suffix c indicates camera coordinate system respectively. The direction of the mapping is from camera c to projector p_i. In addition, we assume e or v indicates eye position, also refer to as *virtual camera*[3), and r denotes the reference coordinate system for later use. The mapping $\boldsymbol{\Psi}_{p_i c}$ is defined in Eq.(1)[1),3).

$$\boldsymbol{x}_{p_i} = \boldsymbol{\Psi}_{p_i c}(\boldsymbol{x}_c)$$
$$\equiv \boldsymbol{H}\boldsymbol{x}_c - \left(\boldsymbol{q}^T\boldsymbol{x}_c \pm \sqrt{(\boldsymbol{q}^T\boldsymbol{x}_c)^2 - \boldsymbol{x}_c^T\boldsymbol{Q}_{33}\boldsymbol{x}_c}\right)\boldsymbol{e}_c \ , \quad (1)$$

where H is a homography matrix between the camera to the projector, T indicates transpose, $\boldsymbol{e}_c$ is an epipole, $\boldsymbol{Q}_{33}$ and $\boldsymbol{q}$ are according to a 4x4 quadric parameter matrix:

$$\boldsymbol{Q} = \begin{bmatrix} \boldsymbol{Q}_{33} & \boldsymbol{q} \\ \boldsymbol{q}^T & 1 \end{bmatrix} \qquad (2)$$

In case of the camera position and eye position do not coincide, a transformation from camera

† Mitsubishi Precision Co., Ltd., Japan.
†† Mitsubishi Electric Research Lab., USA.
††† MIT Media Lab., USA.

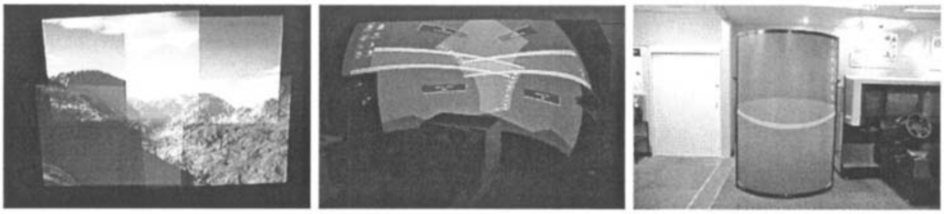

(a) Planar screen: before calibration

(b) Quadric screen (Dome, cut both edges): before calibration

(c) Quadric screen (Cylinder): before calibration

(d) Planar screen : calibrated

(e) Quadric screen (Dome, cut both edges) : calibrated

(f) Quadric screen(Cylinder): calibrated

Fig. 1 Applications of *virtual camera method* to the parametric screen: Example of four projectors, and the automatic intensity correction on the part of overlapped area is carried out.

to eye is calculated mathematically using reference point which is usually a center of the quadric surface. This is a main idea of the *virtual camera method.* Figure 1 shows commercialized several applications of this method.

3. Multiple shots method

Previous calibration methods assume that the camera can observe the entire screen. In the case of large field of view or spherical screens, it is hard to fit the entire screen within a single camera view. In the next Sections, we extended the calibration method to cover the entire screen with several captured images from different locations.

The camera images have an overlapping area which includes part of the projectors' overlapped area as shown in Fig. 2(a) and (b). The captured images with overlapped area can then be used to unify differently reconstructed 3D points into a unified coordinate system. This approach requests several camera shots at different locations and we call the method *multiple shots method.*

The main goal is to calculate mapping functions $\boldsymbol{\Psi}_{ep_i}$: $(i = 1 \cdots I)$ to correct image distortion. At first we calculate $\boldsymbol{\Psi}_{v_s p_i}$: $(s = 1 \cdots S, i = 1 \cdots I)$. In this calculation, the reconstructed screen shape represented with Q in Eq.(2) is used. Then $\boldsymbol{\Psi}_{v_s p_i}$ is transformed into $\boldsymbol{\Psi}_{ep_i}$ using same idea of *virtual camera method.* In following sections, the detailed procedures are described step by step.

3.1 Detection of the screen geometry

(1) Reconstruction of 3D points

Figure 2(b) shows reconstruction of 3D points using a stereo-camera. From projector i, the known 2D points $x^k_{p_i}$ (where k indicates a point in a known pattern: $k = 1 \cdots K$) are projected on the screen. The projected points are captured with the stereo-camera located at c_m, and then reconstructed into 3D points $\boldsymbol{X}^{p_i,k}_{c_m}$ in camera c_m coordinate system. The same procedure is carried out for projector j to get $\boldsymbol{X}^{p_j,k}_{c_m}$. In this procedure, the camera c_m can be located freely as long as the projected pattern of projector p_i and overlapping area with adjacent projector j are included in the camera view. The above procedure is carried out for all projectors to get all 3D points which cover the entire screen.

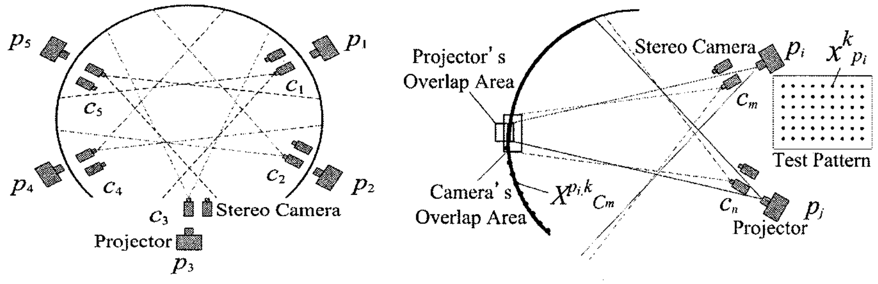

(a) Camera locations : The location and orientation of camera are not necessary to be measured.

(b) Capturing test pattern images of overlapped area by projector p_i and adjacent projector p_j : camera c_n can be allocated freely so as to capture projectors' overlapped area.

Fig. 2 How to position a stereo-camera in multiple shots method: The figure shows example of five projectors display system and a stereo-camera which move appropriately to capture images.

(2)Unification of coordinate systems

To estimate screen geometry, reconstructed 3D points in different coordinate systems corresponding to each camera are unified into a common coordinate system. The unification procedure consists of the following two steps: (a) One of the camera coordinate system c_n is selected arbitrarily as the unified coordinate system. (b) Then each camera coordinate system is transformed to *virtual camera* v_s, located on the extension of diameter line where the whole screen can be observed. We refer to v_s as the *reference virtual camera.*

Step (a): To convert coordinates of 3D points in coordinate system c_m into *reference virtual camera* v_s, the relative orientation $\boldsymbol{R}_{c_n c_m}$ and translation $\boldsymbol{t}_{c_n c_m}$ between cameras are necessary.

The unknown $\boldsymbol{R}_{c_n c_m}$, $\boldsymbol{t}_{c_n c_m}$ can be calculated by minimizing the following constrained Eq.(3):

$$\sum_{k=1}^{K} \left| \boldsymbol{R}_{c_n c_m} \boldsymbol{X}^{p_i,k}_{c_m} + \boldsymbol{t}_{c_n c_m} - \boldsymbol{X}^{p_i,k}_{c_n} \right| \quad (3)$$

$\boldsymbol{X}^{p_i,k}_{c_m}$ and $\boldsymbol{X}^{p_i,k}_{c_n}$ are corresponding 3D points in different coordinate systems.

Step (b): 3D points in each camera coordinate system $\boldsymbol{X}^{p_i,k}_{c_m}$ are then transformed to *virtual camera* coordinate system v_s.

3D points $\boldsymbol{X}^{p_i,k}_{v_s}$ in the unified coordinate system v_s can be calculated by the following equation using known $\boldsymbol{R}_{c_n c_m}$, $\boldsymbol{t}_{c_n c_m}$ calculated in step (a) and known $\boldsymbol{R}_{v_s c_n}$ and $\boldsymbol{t}_{v_s c_n}$ ☆.

$$\boldsymbol{X}^{p_i,k}_{v_s} = \boldsymbol{R}_{v_s c_n} \boldsymbol{R}_{c_n c_m} \boldsymbol{X}^{p_i,k}_{c_m} + \boldsymbol{R}_{v_s c_n} \boldsymbol{t}_{c_n c_m} + \boldsymbol{t}_{v_s c_n} \quad (4)$$

(3) Estimation of the screen geometry

Each 3D points $\boldsymbol{X}^{p_i,k}_{v_s}$ projected by each projector are on the quadric screen so that the unknown matrix $\boldsymbol{Q}_{v_s}$ can be calculated by solving an optimization problem using known 3D points $\boldsymbol{X}^{p_i,k}_{v_s}$ $(k = 1 \cdots K)$:

$$\sum_{i}^{I} \sum_{k}^{K} \left| \boldsymbol{X}^{p_i,k\,T}_{v_s} \boldsymbol{Q}_{v_s} \boldsymbol{X}^{p_i,k}_{v_s} \right| \rightarrow min \quad (5)$$

3.2 Derivation of mapping function

(1) Orientation of each projector

3D points $\boldsymbol{X}^{p_i,k}_{v_s}$ in coordinate system v_s and corresponding 2D points $\boldsymbol{x}^k_{p_i}$ have the following relation:

$$\boldsymbol{x}^k_{p_i} = \boldsymbol{P}_{p_i v_s} \boldsymbol{X}^{p_i,k}_{v_s} , \quad (6)$$

where $\boldsymbol{P}_{p_i v_s}$ represents projective matrix of projector i. Therefore the unknown projective matrix $\boldsymbol{P}_{p_i v_s}$ can be calculated by solving an optimization problem with known $\boldsymbol{X}^{p_i,k}_{v_s}$ and $\boldsymbol{x}^k_{p_i}$:

$$\sum_{k=1}^{K} \left| \boldsymbol{P}_{p_i v_s} \boldsymbol{X}^{p_i,k}_{v_s} - \boldsymbol{x}^k_{p_i} \right| \rightarrow min \quad (7)$$

The projective matrix $\boldsymbol{P}_{p_i v_s}$ is $\boldsymbol{P}_{p_i v_s} = \boldsymbol{K}^{p_i} [\boldsymbol{R}_{p_i v_s} | \boldsymbol{t}_{p_i v_s}]$ and the intrinsic matrix of the projector $\boldsymbol{K}^{p_i}$ are known in advance so

☆ This is because relative location and orientation between v_s and c_n, i.e. $\boldsymbol{R}_{v_s c_n}$ and $\boldsymbol{t}_{v_s c_n}$, can be calculated using *virtual camera method.*

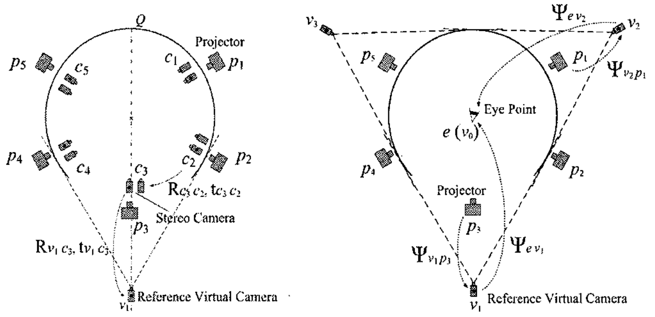

(a) Setting of *reference virtual camera*: The *reference virtual camera* has to be allocated on extension of diameter line to observe whole screen.

(b) Corresponding relation between projector, *reference virtual camera* and eye

Fig. 3 Set up for *virtual camera* and eye position on *Multiple shots method.*

that it can be separated into rotation $\boldsymbol{R}_{p_i v_s}$ and translation $\boldsymbol{t}_{p_i v_s}$.

(2) Calculation of mapping function $\Psi_{v_s p_i}$

At first, $\boldsymbol{Q}_{v_s}$ is transformed into projector p_i coordinate system using calculated $\boldsymbol{R}_{p_i v_s}$ and $\boldsymbol{t}_{p_i v_s}$ as follow.

$$\boldsymbol{Q}_{p_i} = \boldsymbol{M}_{p_i v_s} \boldsymbol{Q}_{v_s} (\boldsymbol{M}_{p_i v_s})^T, \qquad (8)$$

where the 4x4 matrix $\boldsymbol{M}_{p_i v_s}$ is defined as

$$\boldsymbol{M}_{p_i v_s} = \begin{bmatrix} \boldsymbol{R}_{p_i v_s} & \boldsymbol{t}_{p_i v_s} \\ \boldsymbol{0}^T & 1 \end{bmatrix} .$$

The mapping between each projector and *reference virtual camera* $\boldsymbol{\Psi}_{v_s p_i}, (s = 1 \cdots S,\ i = 1 \cdots I)$ is calculated using known projector position $\boldsymbol{R}_{p_i v_s}$, translation $\boldsymbol{t}_{p_i v_s}$ and quadric matrix $\boldsymbol{Q}_{p_i}$ as shown in Eq. (9)[1)3)].

$$\begin{aligned} \boldsymbol{A}_{v_s p_i} &= \boldsymbol{K}^{v_s}(\boldsymbol{R}_{v_s p_i}) - \boldsymbol{e}_{v_s} \boldsymbol{q}_{p_i}^T , \\ \boldsymbol{E}_{v_s p_i} &= \boldsymbol{q}_{p_i} \boldsymbol{q}_{p_i}^T - \boldsymbol{Q}_{33 p_i} , \\ \boldsymbol{e}_{v_s} &= \boldsymbol{K}^{v_s}(\boldsymbol{t}_{v_s p_i}) , \end{aligned} \qquad (9)$$

where, $\boldsymbol{Q}_{33 p_i}$ and $\boldsymbol{q}_{p_i}$ are part of matrix $\boldsymbol{Q}_{p_i}$ (Eq. 2), and $\boldsymbol{K}^{v_s}$ is the intrinsic matrix of the *reference virtual camera.*

(3) Optimization of mapping $\Psi_{v_s p_i}$

The calculated mapping has a variety of errors and can not be applied directly for image distortion. Using computed $\boldsymbol{A}_{v_s p_i}, \boldsymbol{E}_{v_s p_i}, \boldsymbol{e}_{v_s}$ in the previous step as the initial values, we can improve the precision of the parameters by minimizing the following cost function C_{v_s}:

$$C_{v_s} = \sum_k \left| \boldsymbol{x}^k_{v_s} - \hat{\boldsymbol{x}}^k_{v_s} \right| , \qquad (10)$$

where, $\boldsymbol{x}^k_{v_s} = \boldsymbol{P}_{v_s v_s} \boldsymbol{X}^{p_i,k}_{v_s}$ and:

$$\hat{\boldsymbol{x}}^k_{v_s} = \boldsymbol{A}_{v_s p_i} \boldsymbol{x}^k_{p_i} \pm \left(\sqrt{(\boldsymbol{x}^k_{p_i})^T \boldsymbol{E}_{v_s p_i} (\boldsymbol{x}^k_{p_i})} \right) \boldsymbol{e}_{v_s} .$$

The projective matrix $\boldsymbol{P}_{v_s v_s} = \boldsymbol{K}^{v_s}[\boldsymbol{I}|\boldsymbol{0}]$ is a virtual one so that it can be defined mathematically with zero error. In addition, we reconstructed $\boldsymbol{X}^{p_i,k}_{v_s}$ using the stereo-camera so that the virtually projected point $\boldsymbol{x}^k_{v_s}$ has higher accuracy than $\hat{\boldsymbol{x}}^k_{v_s}$. We think that using $\boldsymbol{x}^k_{v_s}$ as a reference is reasonable.

3.3 Actual mapping function Ψ_{ep_i}

As a final step, the mapping $\boldsymbol{\Psi}_{v_s p_i}(s = 1 \cdots S)$ from projector $p_i(i = 1 \cdots I)$ to actual eye e (i.e, v_0) is calculated. Each mapping $\boldsymbol{\Psi}_{v_s p_i}(s = 1 \cdots S, i = 1 \cdots I)$ is already calculated so that if we could find mapping $\boldsymbol{\Psi}_{ev_s}$, then we can calculate actual mapping $\boldsymbol{\Psi}_{ep_i}$ using Eq. (11).

$$\boldsymbol{\Psi}_{ep_i} = \boldsymbol{\Psi}_{ev_s} \boldsymbol{\Psi}_{v_s p_i} \quad (s = 1 \cdots S, i = 1 \cdots I) \qquad (11)$$

Relative position and orientation between *reference virtual camera* and eye can be geometrically calculated using *virtual camera method* so that mapping $\boldsymbol{\Psi}_{ev_s}$ from *reference virtual camera* to eye e, i.e. *reference virtual camera* v_0, is calculated.

In case of 5 projectors shown in Fig. 3, the mappings from each projector to eye are as follows.

(a) Configuration of a cylindrical display system: with 5 projectors

(b) A stereo-camera unit: base line is 50cm long

(c) Cylindrical screen(Diameter:6m, Hight: 3m, FOV:270°)

Fig. 4 Example for the cylindrical display system with large field of view: 5 projectors and 270 degrees field of view. If screen is quadric type, our method can be applied to any type of screen.

$$\begin{array}{l}\Psi_{ep_i} = \Psi_{ev_1}\Psi_{v_1p_i} \quad (i = 2\cdots4) \\ \Psi_{ep_1} = \Psi_{ev_2}\Psi_{v_2p_1}; \quad \Psi_{ep_5} = \Psi_{ev_3}\Psi_{v_3p_5}\end{array} \tag{12}$$

4. Prototyping of display system and evaluation

Table 1 Specifications of large field of view cylindrical display system

No.	Devices	Specifications
(1)	PC	Intel Pentium4 3.6GHz, 3GB WindowsXP SP2
(2)	Network	Gigabit Ethernet
(3)	Camera	2 Sets XGA (1024x768 pixels)
(4)	Projectors	5 Sets: SXGA (1280x1024 pixels) Victor DLA-M2000SC,2000lm
(5)	Graphics	NVIDIA QuadroFX4500 512MB
(6)	Screen	Diameter 6m Height 3m

4.1 Display system

Fig. 4 shows large field of view cylindrical display system being applied the unified calibration method. Overview of the display system is shown in the figure 4(a), Fig. (b) shows outlook of the stereo-camera for calibration, Fig. (c) shows cylindrical screen. The detailed specifications of the system are shown in Table 1. The image generation is carried out in the PC cluster (PC-IG) shown in Fig. 4(a), and the realtime distortion correction is carried out in commodity graphics boards using Cg language[3].

4.2 Evaluation

The evaluation of the unified calibration method for the large field of view using resultant images is shown in Fig. 5. Fig. 5(a) shows projected images before the unified calibration, (b) and (c) show calibration using test pattern. In addition, Fig 5(d)~(f) show a landing scene of actual flight simulator application. The intensity anomaly in overlapping area of adjacent projectors is compensated using alpha map in OpenGL functionality[6]. There are no geometrical discontinuity and distortion as shown in Fig. 5(b), (c).

Table 2 Precision of calibration for each projector

Proj No.	mean error in pixel (Number of points)	Max. error [mm] (Overlapping Proj.No.)
1	0.243(178)	4.0 (1-2)
2	0.221(212)	8.0 (2-3)
3	0.260(218)	12.0 (3-4)
4	0.223(231)	3.0 (4-5)
5	0.292(232)	–

In Table 2, the projection error for corresponding points using mapping function and measured one on the screen for each projector at overlapping area are shown. The listed data for "mean error in pixel" in table 2 show mean value of projection error, i.e. summed result of Eq.(10) is divided by number of points.

According to the actual measurement on the screen, 1 pixel error correspond 6 mm in maximum. As shown in Table 2, current worst error between projectors is less than 2 pixels. Therefore, we think that the error between projectors in worst case is acceptable.

5. Conclusion and future work

In this paper, we described a unified automatic geometrical calibration approach for displays on parametric curved screens. In particular, we showed that even for large field of view display system, we can use a simple pair of cameras and compute geometric and photometric parameters for quadric curved screens. We believe this is a first for a large field of view system. We have successfully built several prototypes with the proposed approach.

(a) Image of before calibration: At center in a part of cockpit, the pilot seat is located.

(b) Image of test pattern after calibration: whole screen is shown

(c) Image of test pattern after calibration: partially magnified

(d) Simulation image (sea and sky): left side of screen is shown

(e) Simulation image (sea and sky): center of the screen is shown

(f) Simulation image (sea and sky): right side of the screen is shown

Fig. 5 An example application of the unified calibration method for large field of view cylindrical display system: The method can be applied to any quadric screen such as spherical screen. The number of projectors can be freely used depending on requested resolution. In this example 5 projectors are used.

Our method can simplify tedious and complex task of installing and maintaining seamless multi-projectors display systems such as spherical display systems used in planetariums or cylindrical displays used in visualization centers.

In the future, we would like to apply maximum likelihood method for optimization of mapping function so that it is robust to screen deviations and image noise.

References

1) RASKAR R., VAN BAAR J., BEARDSLEY P., WILLWACHER T., RAO S., FORLINES C.: iLamps: Geometrically aware and self-configuring projectors, *ACM Transaction on Graphics*, ACM Press, vol. 22, no.3, pp. 809–818, 2003.
2) VAN BAAR J., WILLWACHER T., RAO S., RASKAR R.: Seamless multi-projector display on curved screens, *Proceedings of Eurographics Workshop on Virtual Environments(EGVE)2003*, ACM Press, pp. 281–286, 2003.
3) OGATA M., WADA H., KAJIHARA K., VAN BAAR J.: A multi-projector display system with virtual camera method for distortion correction on quadric surface screens, *IEICE Transactions*, IEICE Transactions on Information and Systems, vol. E89-D, no.2, pp. 814–824, 2006.
4) YAMASAKI M., MINAKAWA T., TAKEDA H., HASEGAWA S., SATO M.: Technology for seamless multi-projection onto a hybrid screen composed of differently shaped surface elements, Proceedings of Sixth International Immersive Projection, Technology Symposium, Orlando, Florida, pp. 1–8, 2002.
5) HASHIMOTO N., KURAHASHI M., SATO M.: Non-distorted image projection method for a multi-projection display with a curved screen, J. Institute of Image Information and Television Engineers(ITE), vol.58, no.4, pp.507–513, 2004.
6) RASKAR R., VAN BAAR J., WILLWACHER T., RAO S.: Quadric transfer for immersive curved screen displays , *Eurographics 2004*, Proc. Eurographics, pp. 451–460, 2004.